Photon Transmission Technique for Studying Film Formation from Polystyrene Latexes Prepared by Dispersion Polymerization Using Various Steric Stabilizers

ÖNDER PEKCAN,[1] ERTAN ARDA,[2] KEMAL KESENCİ,[3] ERHAN PİŞKİN[3]

[1] İstanbul Technical University, Department of Physics, Maslak, 80626, İstanbul, Turkey

[2] Trakya University, Department of Physics, 22030, Edirne, Turkey

[3] Hacettepe University, Chemical Engineering Department and Bioengineering Division, Beytepe, 06532, Ankara, Turkey

Received 19 March 1997; accepted 27 October 1997

ABSTRACT: A photon-transmission method was used to monitor the evolution of transparency during film formation from various polystyrene (PS) particles which were produced using different steric stabilizers, that is, poly(acrylic acid) (PAA), poly(vinyl alcohol) (PVA), and polyvinylpyrrolidone (PVP). The latex films were prepared from PS particles at room temperature and annealed at elevated temperatures in various time intervals above the glass transition (T_g). To simulate the latex film-formation process, a Monte Carlo technique was performed for photon transmission through a rectangular lattice. The number of transmitted (N_{tr}) photons were calculated as a function of particle–particle interfaces that disappeared. The increase in the transmitted photon intensity (I_{tr}) was attributed to the increase in the number of interfaces that disappeared. The Prager–Tirrell (PT) model was employed to interpret the increase in crossing density at the junction surface. The backbone activation energy (ΔE) was measured and found to be around 120 kcal mol^{-1} for a diffusing polymer chain across the junction surface for all PS latex films. © 1998 John Wiley & Sons, Inc. J Appl Polym Sci 68: 1257–1267, 1998

Key words: film formation; photon transmission; polystyrene latexes; stabilizers

INTRODUCTION

Latexes containing monodisperse polymeric particles in the micron-size range (usually between 1 and 10 μm in diameter) can be prepared by dispersion polymerization.[1–6] In a dispersion polymerization process, the reaction mixture starts out as a homogeneous solution containing monomer dissolved in an inert medium, and the resulting polymer precipitates as solid spherical particles, stabilized by a steric stabilizer to form a latex. Several process variables, that is, stabilizer type and concentration, initiator type and concentration, dispersion medium, monomer type and concentration, and temperature affect both the kinetics and yield of polymerization and also the properties of the final product (e.g., particle size, monodispersity, surface charge, and chemistry).[1–14]

Polymer latexes have been utilized in a wide variety of applications in the coating and adhesive technologies, biomedical field, and information industry and in microelectronics. In many of these applications, for example, coatings and adhesives, latexes form thin polymer films on a substrate surface. Properties (mechanical, optical, transport, etc.) of the final film should be tailor-made according to the application.

From a phenomenological point of view, the

Correspondence to: Ö. Pekcan.

Journal of Applied Polymer Science, Vol. 68, 1257–1267 (1998)
 CCC 0021-8995/98/081257-11

film-formation process has traditionally been considered to occur in three sequential stages, namely, "evaporation of the dispersion medium (e.g., water)"; "packaging of deformed particles"; and "formation of a mechanically rigid film." As the dispersion medium evaporates during the film formation, latex particles approach each other and eventually stick, depending on their colloidal stability.[15,16] The obtained dry polymer film is not homogeneous; a memory of the particles still remains at this stage of film formation. The hydrophilic membrane separating the particles has to break in a coalescence step, allowing a direct contact between polymer particles for interdiffusion of the polymer chains. Particle sticking, coalescence, and polymer interdiffusion occur successively depending on the glass transition temperature (T_g) and molecular weight of the polymer and on the nature of the hydrophilic membrane. When annealing the dry film above the T_g, the deformation of particles first leads to void closure,[17,18] then voids disappear and complete welting between particles can be established.

After the void-closure process is completed, the mechanism of film formation, by the annealing of latex films, is known as the interdiffusion of polymer chains followed by healing at the polymer–polymer interface. In general, when two identical polymeric materials are brought into intimate contact and heated at a temperature above the glass transition, the polymer chains become mobile and interdiffusion of the polymer chains across the interface can occur. After this process, the junction surface becomes indistinguishable in all respects from any other surface that might be located in the polymeric material. This process is called the healing of the junction at which the joint achieves the same cohesive strength as that of the bulk polymeric material. The word interdiffusion in polymer science is used for the process of mixing, intermingling, and homogenization at the molecular level, which implies diffusion among the polymer chains. In the bulk state, polymer chains have a Gaussian distribution of segments. Chains confined to the half space adjacent to the junction have distorted conformations.[19–21] Diffusion across the junction leads to configurational relaxation and the recovery of Gaussian chain behavior. Polymers much larger than a certain length are often pictured as confined to a tube, and diffusion occurs by a reptile motion.[17] In this model, each polymer chain is considered to be a tube, along the length of which it executes a random back-and-forth motion. This reptilelike motion will cause the chain to slip out of a section of the tube at one end or the other. The reptation time (T_R) describes the time necessary for a polymer to diffuse a sufficient distance for all memory of the initial tube to be lost. This is the time it takes for the initial configuration to be forgotten and the first relaxation to be completed.

Small-angle neutron scattering (SANS) has been used to study latex film formation at the molecular level. Extensive studies using SANS were performed by Sperling and coworkers on compression-molded polystyrene film.[22] The direct-nonradiative energy transfer (DET) method was employed to investigate the film-formation processes from dye-labeled polymeric particles.[23–25] The steady-state fluorescence (SSF) technique combined with DET was recently used to examine the healing and interdiffusion processes in dye-labeled PMMA latex systems.[26–30]

In this study, polystyrene (PS) latices were produced by dispersion polymerization of the monomer (styrene) in an ethanol/water mixture. Poly(acrylic acid) (PAA), poly(vinyl alcohol) (PVA), or polyvinylpyrrolidone (PVP) were used as steric stabilizers with a disperse-phase soluble initiator (i.e., AIBN). Transparencies of the films formed from these PS latexes were studied by measuring the transmitted photon intensities (I_{tr}) using a UV-visible spectrophotometer. Monte Carlo simulations were performed to calculate the transmitted (N_{tr}) photon intensities to simulate the latex film-formation process. The method developed by Prager and Tirrell (PT)[20] was employed to investigate the healing processes at the junction surfaces.

EXPERIMENTAL

Preparation of Monosize PS Latexes

The monomer, styrene (S; Yarpet A : S, Istanbul, Turkey) was treated with aqueous NaOH to remove the inhibitor and stored in a refrigerator until use. The initiator was 2,2-azobisisobutyronitrile (AIBN; BDH Chemicals Ltd., London, UK). Ethyl alcohol (Merck, Frankfurt, Germany)/water mixtures were used as the dispersion medium. Poly(acrylic acid) (PAA) (MW: 450,000, Aldrich, Milwaukee, USA), poly(vinyl alcohol) (PVA) (MW: 50,000, Aldrich), and polyvinylpyrrolidone (PVP) (60,000, Fluka, Zurich, Switzerland) were used as steric stabilizers.

Polymerizations were carried out in a magnetic-driven, sealed, cylindrical reactor equipped with a temperature-control system.[12,13] Two

grams of the steric stabilizer was dissolved in the dispersion medium containing 180 mL of ethyl alcohol and 20 mL of water. The monomer phase was prepared by dissolving 0.28 g AIBN in 20 mL of styrene. These two phases were mixed and charged to the reactor agitated with an anchor-type agitator at a speed of 150 rpm, and the polymerization was conducted at 80°C for 24 h.

The PS latex was cleaned first using a serum replacement as also given in our previous publications.[12,13] The latex from the reactor was centrifuged and the supernatant was removed. The particles were washed with fresh dispersion medium a few times, then distilled water was added and a new dispersion was stirred for 24 h at room temperature to remove any stabilizer remaining on the surface of the polymeric particles. The PS latex was treated with a mixed bed of anion- and cation-exchange resins (H^+ and OH^- type, Amberlite, BDH) at the last step.

The average particle size of each type of PS particle was evaluated using scanning electron micrographs. The latex solution was spread onto a metal disk and the solvent (i.e., water and alcohol) was evaporated. The dried beads were coated with a thin layer of gold (about 100 Å) in a vacuum. Three separate photographs (each containing 100–300 beads) were taken for each latex sample with 2000–2600 magnification using a scanning electron microscope (SEM, JEOL, JEM1200EX, Japan). The size of the beads was measured on photographs and checked using calibration samples.

The average molecular weights of the PS produced with different stabilizers were determined by a GPC system (Waters, USA). The GPC unit, consisting of a Waters Model 510 HPLC pump and a Waters U6K injector, was equipped with two Ultrastryagel columns (Waters, 10 and 500 Å) in series and a Waters 486 tunable absorbance detector. Chloroform was used both as the solvent and the eluent. Elution was performed at a temperature of 30°C and at a flow rate of 1 mL/min, using a Waters 510 HPLC pump. The columns were calibrated with PS standards (Shodex Standards, SL-105, Showa Denko, Japan).

Film Preparation and UVV Measurements

Films were prepared from the PS latexes prepared with three different stabilizers, that is, PAA, PVA, and PVP, by placing different numbers of drops of the latex on glass plates (with a size of 0.9×3.2 cm^2) and allowing the water to evaporate at room temperature. Here, we were careful to ensure that the liquid dispersion from the droplets covers the whole surface area of the plates and remains there until the water has evaporated. Samples were weighed before and after the film casting to determine the film thicknesses. The average size for the particles was taken to be 2 μm, which was determined from the SEM micrographs, to calculate the number of layers of the films.

In this work, UV-visible (UVV) experiments were carried out with annealed latex film samples. The annealing process of the latex films was performed above the T_g of PS after the evaporation of water, in 5-, 10-, and 15-min time intervals at elevated temperatures between 100 and 155°C. The temperature was maintained within ±1°C during annealing. After annealing, transmissions of the films were detected with a UVV spectrophotometer (Lambda 2S of Perkin–Elmer, USA) at a wavelength between 300 and 400 nm at room temperature. A glass plate was used as a standard for all UVV experiments.

Table I Average Particle Size and Molecular Weights of PS Produced with Different Stabilizers

Stabilizer Type	Particle Diameter (μm)	M_n
PVA	2.02 ± 0.05	1.54×10^4
PVP	2.10 ± 0.03	1.78×10^4
PAA	1.98 ± 0.07	2.47×10^4

RESULTS AND DISCUSSION

PS Latexes

In this study, PS latexes were produced by dispersion polymerization of S in a medium composed of an ethanol/water mixture using steric stabilizers. PAA, PVA, or PVP were used as the steric stabilizers with a disperse-phase-soluble initiator (i.e., AIBN). With the recipe used, monosize PS particles with an average diameter of around 2.0 μm were obtained (Table I). Figure 1 gives a representative SEM micrograph of these particles.

The number-average molecular weights (M_n) of PS produced with different stabilizers, which were determined using the GPC data, are given in Table I. As seen here, the average molecular

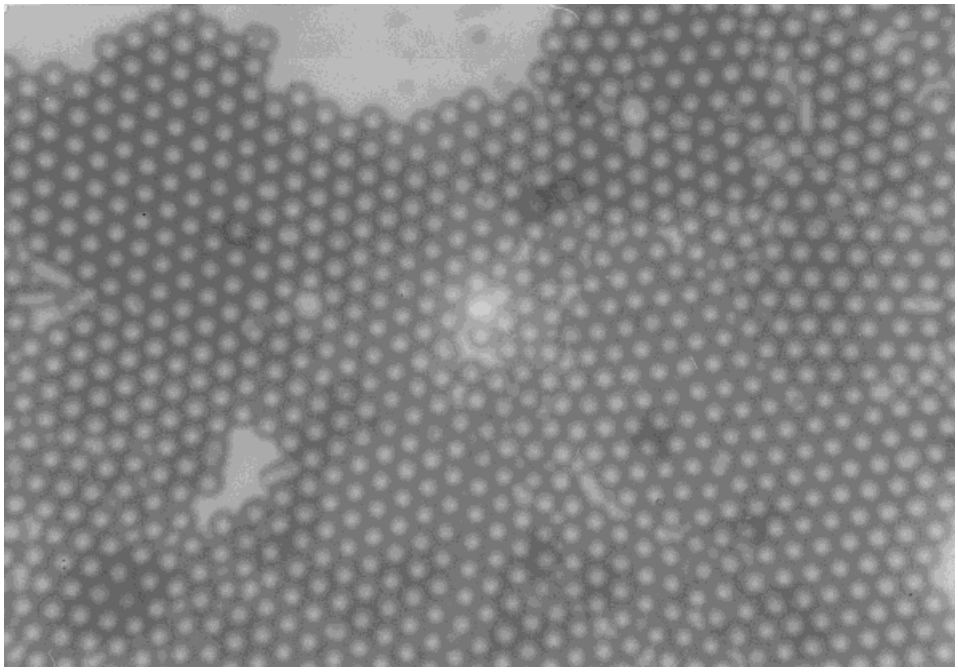

Figure 1 A representative SEM micrograph of PS particles produced in this study.

weights of the PS were in the same order but changed with the stabilizer type, as expected.

Note that, in this study, the type of stabilizer was selected as the critical parameter of focus. It is known that the stabilizer plays an important role in the dispersion polymerization process.[8–14] The stabilizer determines both the particle stability during the particle-formation step and the viscosity of the continuous medium. A graft copolymer (i.e., polymeric stabilizer-*g*-PS) can be formed *in situ* during the particle-formation stage when a precursor polymer (i.e., PVP, PAA, or PVA) that contains proper active sites for chain transfer of the oligomeric radicals is used as a stabilizer. The formation of a graft copolymer during the dispersion polymerization is a complex process. The structure and concentration of the precursor polymer control the rate of formation, concentration, and the properties of the graft copolymer. The formed graft copolymer and the precursor polymer are both adsorbed competitively onto the surface of the resultant polymer particles. Note that the adsorption of the stabilizer molecules on the particle surfaces is described as the physical adsorption, which is rather weak and reversible, which means they can be removed from the surface by a careful cleaning procedure. However, the adsorption of the graft copolymer (which carries the stabilizer molecules) is termed anchorage adsorption (including chemical bound and strongly entrapped graft copolymer molecules on the surface), which means that these molecules cannot easily be removed from the particle surfaces.

From the above discussion, one can easily draw the conclusion that the surface chemistry of the PS latex particles would be different when one uses different stabilizer molecules in the dispersion polymerization. This also means that the film formation of the latexes carrying different stabilizer molecules (most probably chemically attached) on their surfaces would be different, which was the main question to be addressed in this study. The results related to film formation of these latexes are discussed in the following sections. Note that, for convenience, the films formed from the PS latexes prepared with different stabilizers are called by the stabilizer name, that is, "the PAA, PVA or PVP films," in the rest of this article.

Transparency of Latex Films

Transmitted photon intensities from the PAA, PVA, and PVP films are plotted versus annealing temperature for various time intervals in Figure 2(A–C), respectively. It is seen that all I_{tr} intensity curves start to increase around 110°C, which is above the T_g (105°C) of PS with increasing annealing temperature, and reached a plateau

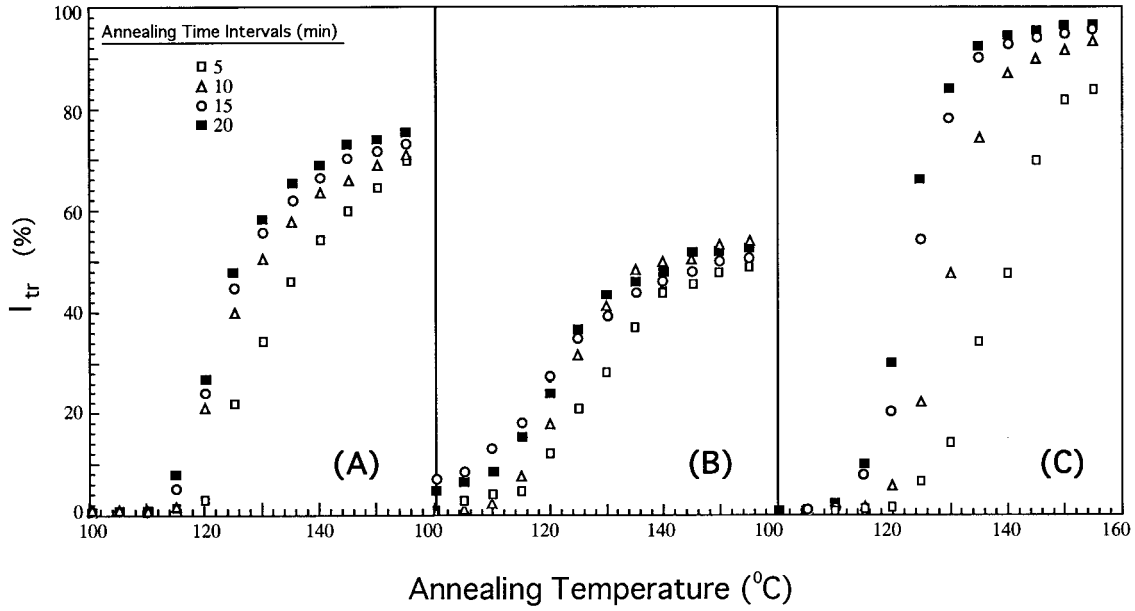

Figure 2 Plot of transmitted photon intensity I_{tr} versus annealing temperature for the latex films: (A) PAA; (B) PVA; (C) PVP.

around 150°C. Relatively small I_{tr} intensities are observed in latex films annealed at short time intervals (2.5 and 5 min), indicating that some photons dissipate, that is, they cannot reach the photodiode after they pass through these films. It was observed that by increasing the annealing time from 10 to 15 to 20 min I_{tr} becomes larger. These changes in the I_{tr} may be interpreted as that annealing the films for longer times results in the formation of more transparent films.

It can be seen from Figure 2 that PVP films can form 95% transparent films when they are annealed around 150°C for 20 min. However, PAA and PVA films can form only 76 and 54% transparent films, respectively, when they are annealed around the same temperature for 20 min. Figure 3 shows a comparison of the transparency of PVP, PVA, and PAA films for 10 min of annealing as a function of annealing temperature where the I_{tr} of the PVA and PAA films present at least 40% smaller values than those of the PVP film.

The transparency of the films can be explained by knowing that homogeneous media do not scatter light. In other words, lattice heterogeneities cause the scattering of light as a result and the transmitted photon intensity decreases in heterogeneous latexes compared to homogeneous ones. As shown in Table I, the average diameters of all PS latexes were very close to each other and were around 2 μm. Therefore, the difference in the extent of homogeneity of the three films mentioned above cannot result from the size differences of the latex particles. Table I also shows that the average molecular weights of the PS produced with different stabilizers are different. If we consider only the molecular weights, we expect the highest transparency from the latex prepared with PVA, which has the lowest molecular weight. Here, we assume that short polymer chains move more easily than do longer chains, which leads to faster coalescence of the particles and, therefore, better transparency. However, this is not the case here. The average chain length of PVP (which forms a more homogeneous film) is between the chain lengths of the other two (which form more heterogeneous films). Therefore, the variation in homogeneities of the latex films cannot be due only to the differences in the average molecular weights of PS. We can also consider the effects of T_g values of the stabilizer molecules which are located at the surface of the particles. The T_g values of PVP, PVA, and PAA are 327, 358, and 379 K, respectively.[31] The particles prepared with PVP have the lowest T_g, which may lead to easier coalesence of the particles and resulting films with higher transparencies, as we obtained. However, when we compare the film formation in the cases of PVA and PAA, the same argument is not valid. The average molecular weight of PS particles prepared with PVP is the lowest and the T_g of PVA is less than that of PAA. Therefore, one expects better transparency in the case of PVA,

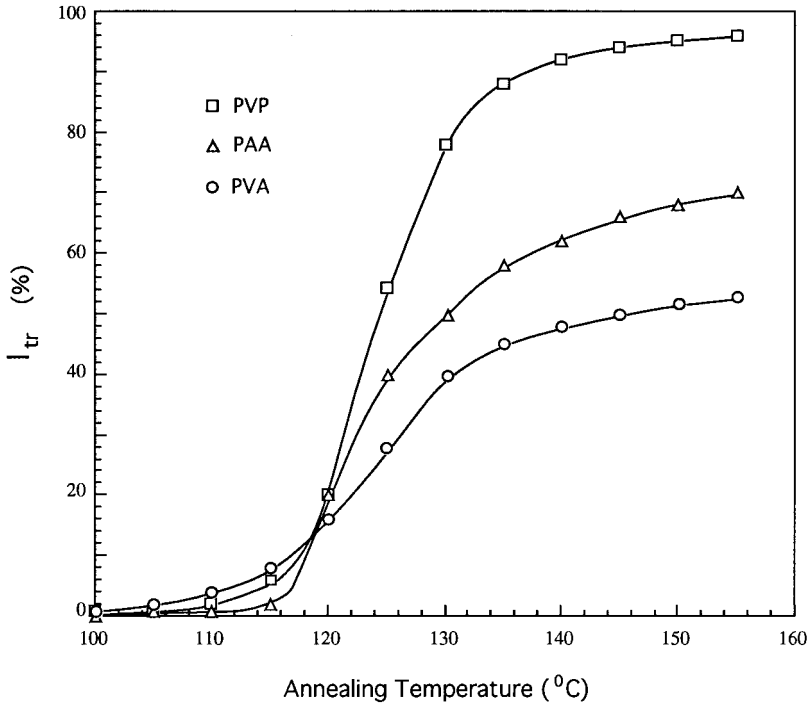

Figure 3 Plot of transmitted photon intensity I_{tr} versus annealing temperature for the PAA, PVA, and PVP films annealed for 10 min.

but this is not the case. One further explanation may be the compatibility of these polymeric stabilizers with the forming PS chains during the dispersion polymerization. The solubility parameters obtained by different methods for PS, PAA, PVA, and PVP are 8.5–9.1, 9.4–10.1, 12.6, and 10.1–11.8 $(\text{cal/cm}^3)^{1/2}$, respectively.[10,31–35] As seen here, the solubility parameter of PAA is closer to that of PS than to the others; in other terms, PAA is more compatible with PS than, especially, PVA. Higher compatibility may result in particle surfaces where more PS molecules may be located on the surface (in parallel, more stabilizer molecules penetrate from the surface to the bulk). Because of this, the particles prepared with PAA form films with higher transparencies than those prepared with PVA. We may conclude this discussion by saying that polymeric particles with smaller average molecular weights, prepared with more compatible stabilizers with lower T_g values, form films with high transparencies.

Monte Carlo Simulations

To interpret the temperature behavior of I_{tr} intensities, a simple rectangular lattice model is used to simulate the latex film-formation process. A rectangular lattice is divided into squares with a side length and the centers of the squares are taken as refraction centers for photons traveling in the lattice. The distance of a photon between each consecutive collision is defined as the mean free path, $\langle r \rangle$, of a photon during its journey in the lattice. Boundaries between squares are randomly removed to simulate the disappearance of particle–particle interfaces during the annealing process of the film. The thickness of the rectangle, d, is taken as 20 in arbitrary units. The direction of the incident photon is taken perpendicular to the film's front surface and the periodic boundary conditions are applied to the motion of a photon (i.e., photons are not allowed to escape from the sides of the lattice). When a photon travels in the rectangular lattice, it always controls the boundary against its moving direction. If there is a boundary, then the photon refracts with a probability of 0.25 to one of the four directions. If there is no boundary against its moving direction, the photon travels with a probability of 1. In this picture, the early stage of annealing can be simulated by a rectangular lattice where a photon has short $\langle r \rangle$. As more boundaries are removed between the square compartments in the lattice, $\langle r \rangle$ values increase, which simulates the latter stage of annealing. As boundaries are continuously removed, $\langle r \rangle$ values increase and more photons can

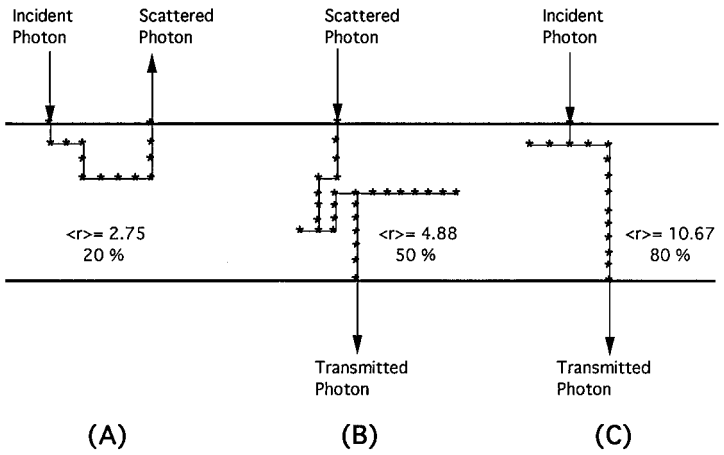

Figure 4 Path of photons in the rectangular latexes when (A) 20%, (B) 50%, and (C) 80% of boundaries between square compartments are removed. The mean free paths, $\langle r \rangle$, of the photons are presented at the corresponding latexes. Dots represent the refraction centers for photons in the rectangular lattice.

be transmitted from the lattice, indicating that annealing causes high transparency. The number of incident photons are taken as 3×10^3 for a good statistic and the number of photons transmitted from the back surface is abbreviated N_{tr}.

Figure 4(A–C) illustrates the path of photons in the corresponding rectangular latexes for short ($\langle r \rangle = 2.75$), medium ($\langle r \rangle = 4.88$), and large ($\langle r \rangle = 10.67$) mean free paths, respectively. Figure 4(A) presents a lattice which simulates the early stage of annealing where 20% of the boundaries are removed and the $\langle r \rangle$ value is very short; as a result, photons can be scattered (remitted) from the front surface of the lattice. Figure 4(B,C) presents latexes with medium and large $\langle r \rangle$ values, where 50 and 80% of boundaries are removed, respectively. In these latexes, photons can be transmitted from the back surface of the latexes. In other words, as more boundaries are removed, more photons can be transmitted from the lattice.

Figure 5 present the plots of the transmitted (N_{tr}) number of photons against the percent of disappeared boundaries between squares in the lattice where the numbers on each N_{tr} curve indicate the percent of trap centers in the lattice. These trap centers which cause the dissipation of photons are placed randomly at the center of the squares. In Figure 5, it can be seen that as the boundaries between the squares are removed N_{tr} increases, which corresponds to an increase in the transparency of the latex film as it is annealed. Here, N_{tr} curves with high trap centers (15 and 23%) may correspond to PVA and PAA latex films where many photons are dissipated due to the low transparency of these films. However, the N_{tr} curve with low trap centers (7%) in Figure 5 may correspond to PVP latex film which presents a high transparency. One notices that the similarities between the curves presented in Figure 5 and in Figure 3 (before saturation) suggests that as the annealing temperature is increased the number of interfaces between the particles decreases, and as a result, I_{tr} increases. Here, even though all

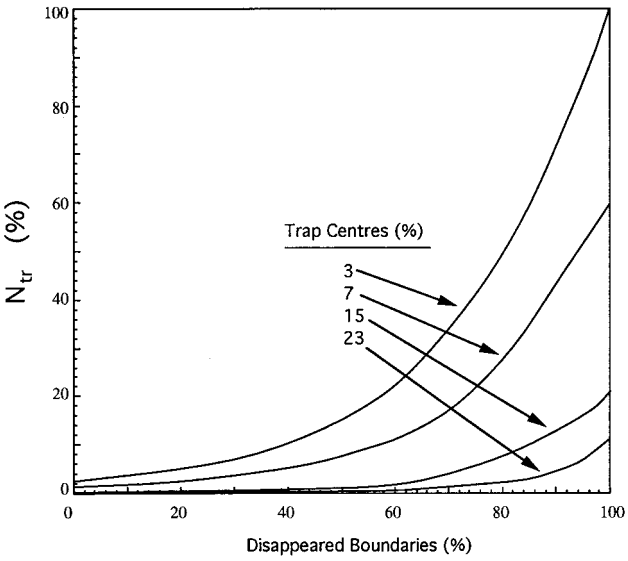

Figure 5 Plot of number of transmitted (N_{tr}) photons versus percent of disappeared boundaries in a rectangular lattice. The number of incident photons is taken as 3×10^3.

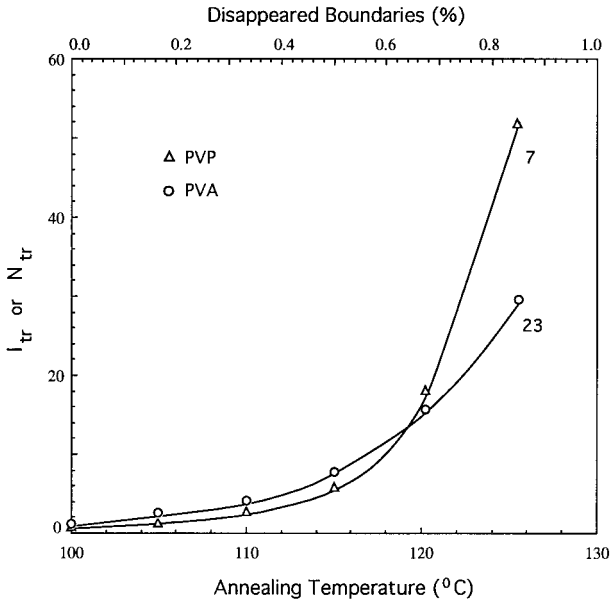

Figure 6 Comparison of I_{tr} data of PVP and PVA for 10-min annealing with the N_{tr} curves for a 7 and 23% trap center, respectively, as a function of annealing time.

the interfaces between the particles are removed, PVA and PAA films exhibit lower transparencies than those of the PVP film, that is, PVA and PAA films cannot attain complete homogeneity due to the incompatibilities between PS and PVA and PAA stabilizers. Most probably, phase separation occurs between these polymeric materials and the domain sizes of these two phases are on the order of the wavelength of light and scatter light, tremendously giving opacity to these latex films. On the other hand, high compatibility between PS and PVP produces nicely homogeneous latex films after all the particle–particle interfaces have disappeared. Figure 6 compares the I_{tr} data of PVP and PVA in Figure 3 with the N_{tr} curves for 7 and 23% tarp centers, respectively, where a good agreement between simulation and experiments can be observed.

Crossing Density and Activation Energies at Junction Surface

When film samples were annealed at elevated temperatures for various time intervals, a continuous increase in I_{tr} intensities was observed until they become saturated. The increase in I_{tr} was already explained in the previous section, by the increase in the transparency of the latex film due to the disappearance of particle–particle interfaces. As the annealing temperature is increased, some part of the polymer chains may cross the junction surface and particle boundaries start to disappear, and as a result, the transmitted photon intensity I_{tr} increases.

To quantify these results, the Prager–Tirrell (PT) model[20] for the chain crossing density was employed. These authors used de Gennes' "repetation" model[19] to explain the configurational relaxation at the polymer–polymer junction where each polymer chain is considered to be confined to a tube in which it executes a random back-and-forth motion. A homopolymer chain with N freely jointed segments of length L was considered by PT, which moves back and forth by one segment with a frequency ν. In time, the chain is displaced down the tube by a number of segments, m. Here, $\nu/2$ is called the "diffusion coefficient" of m in a one-dimensional motion. PT calculated the probability of the net displacement with m during time t in the range of $n - \Delta$ to $n - (\Delta + d\Delta)$ segments. A Gaussian probability density was obtained for small times and large N. The total "crossing density" $\sigma(t)$ (chains per unit area) at the junction surface then was calculated from the contributions due to chains still retaining some portion of their initial tubes, plus a remainder, $\sigma_1(t)$. Here, the $\sigma_2(t)$ contribution comes from chains which have relaxed at least once. Figure 7 shows the cartoon representation of the σ_1 and σ_2 contributions at the particle–particle boundary before and after the disappearance of the interface. In terms of reduced time $\tau = 2\ \nu t/N^2$, the total crossing density can be written as

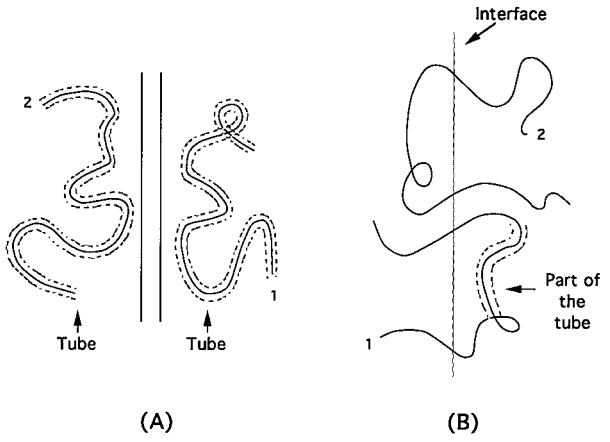

Figure 7 The behavior of chains in the PT model at (A) the particle–particle junction and (B) the disappearing interface. (1) shows a chain still retaining some portion in its initial tube and (2) represents a chain relaxed at least once.

$$\sigma(\tau)/\sigma(\infty) = 2\pi^{-1/2}\Big[\tau^{1/2} + 2\sum_{k=0}^{\infty}(-1) \times n[\tau^{1/2}\exp(-K2/\tau) - \pi^{-1/2}erfc(K/\tau^{1/2})]\Big] \quad (1)$$

For small values, the summation term in the above equation is very small and can be neglected, which then results in

$$\sigma(\tau)/\sigma(\infty) = 2\,\pi^{-1/2}\tau^{1/2} \quad (2)$$

This was predicted by de Gennes on the basis of scaling arguments. To compare our results with the crossing density of the PT model, the temperature dependence of $\sigma(\tau)/\sigma(\infty)$ can be modeled by taking into account the following Arrhenius relation for the linear diffusion coefficient:

$$\nu = \nu_0\exp(-\Delta E/kT) \quad (2)$$

Here, ΔE is defined as the activation energy for the back-and-forth motion. Combining eqs. (2) and (3), a useful relation is obtained as

$$\sigma(\tau)/\sigma(\infty) = R\,\exp(-\Delta E/2kT) \quad (4)$$

where $R = (8\,\nu_0 t/N^2)^{1/2}$ is a temperature-independent coefficient.

The increase in I_{tr} is already related to the disappearance of particle–particle interfaces, that is, as annealing temperature is increased, more chains relaxed across the junction surface, and as a result, the crossing density increased. Now, if it can be assumed that I_{tr} is proportional to the crossing density $\sigma(T)$, then a phenomenological equation can be written as

$$I_{tr}(T)/I_{tr}(\infty) = R\,\exp(-\Delta E/2kT) \quad (5)$$

Logarithmic plots of I_{tr} versus T^{-1} are presented in Figure 8(A–C) for PAA, PVA, and PVP films annealed each for 10 min. The activation energies, ΔE, are produced by fitting the data to eq. (5) and are listed in Table II. These ΔE values are large enough to be responsible for the translational motion of a polymer chain and can be attributed to the backbone motion. Here, the observed ΔE values are found to be strongly dependent on the molecular weight of the PS chains in each particle. ΔE values were obtained for the films prepared with higher molecular weight PS stabilized by PAA: (2.47×10^4) of PS in the particle causes a high ΔE value, that is, PS chains need 203.76 kcal/mol for interdiffusion to form a film. The lower molecular weight (1.54×10^4) of PS chains stabilized with PVA use less energy to move their center of mass across the junction surface to form a similar film. PS chains stabilized with PVP particles with a molecular weight of 1.78×10^4 need the intermediate energy (ΔE) of 150.59 kcal/mol to form a homogeneous latex film.

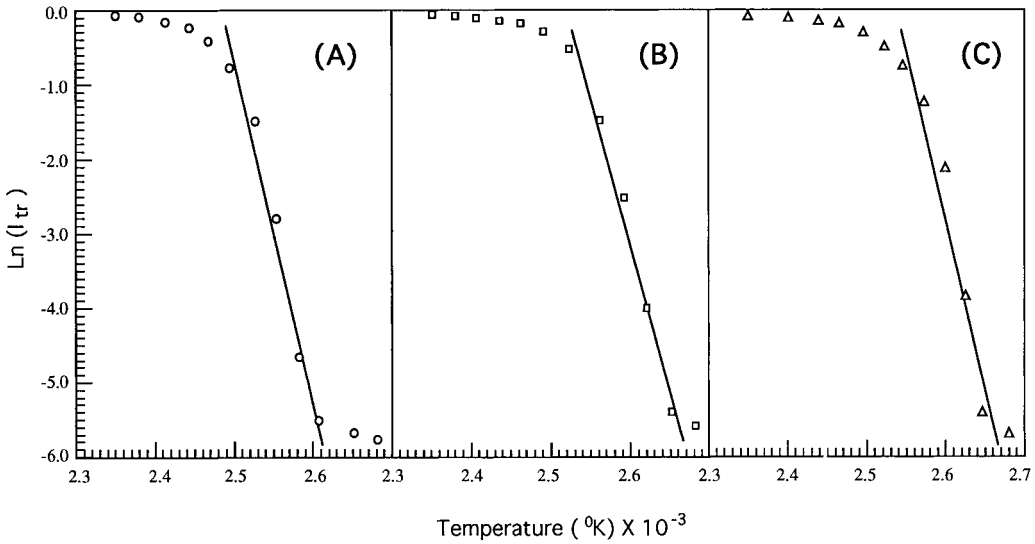

Figure 8 Logarithmic plots of I_{tr} data from Figure 2 versus inverse annealing temperature (T^{-1}) for (A) PAA, (B) PVA, and (C) PVA for 10-min annealing times. Data are fitted to eq. (5) to produce ΔE values.

Table II Experimentally Observed ΔE Values in Various Time Intervals of Annealing

	Time (min)					
Particle	2.5	5.0	10.0	15.0	20.0	
PVP (1.78×10^4)	144.7	155.39	146.71	155.55		150.59
PAA (2.47×10^4)		203.65	207.23	202.22	201.93	203.76
PVA (1.54×10^4)		67.21	91.69	52.03	46.84	64.44

ΔE values were found by fitting the I_{tr} data to eq. (5). Energy units are in kcal/mol. The last column gives the average ΔE values. The molecular weight of PS in each particle are given in the parentheses.

It has to be noted that the observed ΔE values are independent of the time interval in which the latex film is annealed. Strong phase separation during the film formation from PVA particles produces highly scattered ΔE values. It is well known that the backbone activation energy is responsible for the motion of the center of mass of the chain; here, it is reasonable to accept that the σ_2 term of the crossing density contributes to the disappearance of interfaces during the latex film formation. In other words, chains which have relaxed at least once are more responsible for the disappearance of particle–particle boundaries at this temperature range than are the chains still retaining some portions in their initial tubes (σ_1 term).

CONCLUSIONS

In conclusion, in this work, we used a very simple method (UVV) and a model (PT) to calculate the backbone activation energies for interdiffusing polymer chains during film formation from PS latexes. Here, it observed that the PVP stabilizer forms more homogeneous PS films than do films prepared using the PAA and PVA stabilizers. This phenomenon was explained by considering the average molecular weight of PS, the T_g values of the stabilizers, and also the compatibility of PS with these polymeric stabilizers. On the other hand, ΔE values were found to be dependent on the type of stabilizer used. Here, we have to note that for very short annealing time intervals (2.5 and 5 min) the range of temperature slightly moves to the higher values, even though the slopes produce similar ΔE values with the samples annealed at longer time intervals (20, 15, and 10 min). Monte Carlo simulations for the photon transmission from a rectangular lattice also suggested that the particle–particle boundaries disappear by annealing the latex powder, which produces a transparent film.

We thank Professor Taner Oskay for helping us with his stimulating ideas.

REFERENCES

1. K. E. J. Barrett, *Br. Polym. J.,* **5,** 259 (1973).
2. K. E. J. Barrett, Ed., *Dispersion Polymerization in Organic Media* (Wiley, London, 1975).
3. Y. Almog and M. Levy, *J. Polym. Sci.,* **18,** 1 (1980).
4. Y. Almog, S. Reich, and M. Levy, *Br. Polym. J.,* **14,** 131 (1982).
5. K. P. Lok and C. K. Ober, *Can. J. Chem.,* **63,** 209 (1985).
6. C. K. Ober and K. P. Lok, *Macromolecules,* **20,** 268 (1987).
7. C. M. Tseng, Y. Y. Lu, M. S. El-Aasser, and J. W. Vanderhoff, *J. Polym. Sci. Polym. Chem. Ed.,* **24,** 2995 (1986).
8. A. J. Paine, W. Luymes, and J. McNulty, *Macromolecules,* **23,** 3104 (1990).
9. A. J. Paine, *J. Coll. Int. Sci.,* **138,** 157 (1990).
10. A. J. Paine, Y. Deslandes, P. Gerroir, and B. Henrissat, *J. Coll. Int. Sci.,* **138,** 170 (1990).
11. S. Shen, E. D. Sudol, and M. S. El-Aasser, *J. Polym. Sci. Polym. Chem.,* **31,** 1393 (1993).
12. A. Tuncel, R. Kahraman, and E. Pişkin, *J. Appl. Polym. Sci.,* **50,** 303 (1993).
13. A. Tuncel, R. Kahraman, and E. Pişkin, *J. Appl. Polym. Sci.,* **51,** 1485 (1993).
14. S. Shen, E. D. Sudol, and M. S. El-Aasser, *J. Polym. Sci. Polym. Chem.,* **32,** 1087 (1994).
15. S. T. Eckersly and A. Rudin, *J. Coat. Technol.,* **62,** 780 (1990).
16. M. Joanicot, K. Wong, J. Maquet, Y. Chevalier, C. Pichot, C. Graillat, P. Linder, L. Rios, and B. Cabane, *Prog. Coll. Polym. Sci.,* **81,** 175 (1990).
17. P. R. Sperry, B. S. Snyder, M. L. O'Downd, and P. M. Lesko, *Langmuir,* **10,** 2619 (1994).
18. J. K. Mackenzie and R. Shutlewort, *Proc. Phys. Soc.,* **62,** 838 (1946).

19. P. G. de Gennes, *C. R. Acad. Sci. (Paris),* **291,** 219 (1980).
20. S. Prager and M. Tirrell, *J. Chem. Phys.,* **75,** 5194 (1981).
21. Y. H. Kim and R. P. Wool, *Macromolecules,* **16,** 115 (1983).
22. K. D. Kim, L. H. Sperling, and A. Klein, *Macromolecules,* **26,** 4624 (1993).
23. Ö. Pekcan, M. A. Winnik, and M. D. Croucher, *Macromolecules,* **23,** 2673 (1990).
24. Y. Wang, C. L. Zhao, and M. A. Winnik, *J. Chem. Phys.,* **95,** 2143 (1991).
25. Y. Wang and M. A. Winnik, *Macromolecules,* **26,** 3147 (1993).
26. M. Canpolat and Ö. Pekcan, *J. Polym. Sci. Polym. Phys. Ed.,* **34,** 691 (1996).
27. M. Canpolat and Ö. Pekcan, *Polymer,* **36,** 4433 (1995).
28. Ö. Pekcan, *Trends Polym. Sci.,* **2,** 236 (1994).
29. M. Canpolat and Ö. Pekcan, *Polymer,* **36,** 2025 (1995).
30. Ö. Pekcan and M. Canpolat, *J. Appl. Polym. Sci.,* **59,** 1699 (1996).
31. J. Brandrup and E. H. Immergut, *Polymer Handbook,* 3rd ed., New York, 1989.
32. A. G. Shvart, *Kolloid Zh.,* **18,** 755 (1956).
33. D. Mangaraj, S. Patra, and S. B. Rath, *Macromol. Chem.,* **67,** 84 (1963).
34. C. Lety-Sistel, B. Seblle, and C. Quivoron, *Eur. Polym. J.,* **9,** 1297 (1973).
35. M. Şen and O. Güven, *J. Polym. Sci. Polym. Phys.,* to appear.